Vol 17 No 10, October 2008
1674-1056/2008/17(10)/3792-07

Chinese Physics B

Mode coupling in nonlinear Kelvin–Helmholtz instability*

Wang Li-Feng(王立锋)[a], Ye Wen-Hua(叶文华)[b)c)†],
Li Ying-Jun(李英骏)[a], and Meng Li-Min(孟立民)[a]

[a] *China University of Mining and Technology, Beijing* 100083, *China*
[b] *Institute of Applied Physics and Computational Mathematics, Beijing* 100088, *China*
[c] *Department of Physics, Zhejiang University, Hangzhou* 310028, *China*

(Received 28 January 2008; revised manuscript received 12 March 2008)

This paper investigates the interaction of a small number of modes in the two-fluid Kelvin–Helmholtz instability at the nonlinear regime by using a two-dimensional hydrodynamic code. This interaction is found to be relatively long range in wave-number space and also it acts in both directions, i.e. short wavelengths affect long wavelengths and vice versa. There is no simple equivalent transformation from a band of similar modes to one mode representing their effective amplitude. Three distinct stages of interaction have been identified.

Keywords: Kelvin–Helmholtz instability, mode coupling, numerical simulation
PACC: 5235, 4720, 5235M, 4735

1. Introduction

Kelvin–Helmholtz (KH) instability arises in a horizontally stratified heterogeneous fluid when the different layers are in relative motion.[1] The resulting instability is of great importance in many astrophysical and geophysical situations such as the interaction of the solar wind with the earth's magnetosphere,[2] the jets in nuclei extragalactic radio sources,[3,4] supernovae explosions,[5−7] the merger of a binary neutron star system,[8] etc.

There are a number of studies about the single-wavelength sinusoidal perturbation of the interface between the fluids.[9−11] If the initial perturbation amplitude η_0, is much smaller than the wavelength λ, the perturbation grows exponentially in time. As the amplitude of the instability becomes larger, nonlinear effects become important and a great deal of higher harmonics is initiated.[12,13] The nonlinear evolution of single-mode KH instability has been investigated analytically[14−16] for the weakly nonlinear stage, experimentally for nonlinear stage[17,18] and computationally for both weakly and fully nonlinear stage.[19,20] However, mode coupling is not so clear and in most physical cases the flow cannot be described by a single mode. It is important to investigate the mode coupling in the KH instability especially the nonlinear regime.

Broadly speaking, we distinguish among three phases in the evolution of a KH system. Phase I is the linear regime, when the flow is described adequately by a linear superposition of the perturbing modes. In phase II nonlinear effects become significant but the system can still be analysed in terms of the perturbing modes. In phase III the flow has developed into a highly disordered regime.

In Section 2 we will briefly introduce the mode coupling model theoretically. In Section 3 we will shortly describe the two-dimensional hydrodynamic code and the method. Then, in Section 4, we shall first demonstrate mode coupling that occurs during the second phase of flow evolution, where nonlinear interaction between modes is already present but principal modes can still be identified in the mode spectrum. The evolution of a combination of modes will be compared to the single-mode evolution (when only one mode is initially present). The interaction is not expected to be symmetric in wave-number space. We summarize the work in Section 5.

2. Mode coupling model

At the interface ($F(\boldsymbol{r}, t) = 0$) of two layer incompressible fluid, the continuous condition of pressure

*Project supported by the Research Fund for the Doctoral Program of Higher Education of China (Grant No 20070290008) and the National Basic Research Program of China (Grant No 2007CB815100).
†Corresponding author. E-mail: ye_wenhua@iapcm.ac.cn

can be written as[21]

$$\rho_1\left\{\frac{\partial\Phi_1}{\partial t}+\frac{1}{2}(\nabla\Phi_1)^2+f_1(t)\right\} = \rho_2\left\{\frac{\partial\Phi_2}{\partial t}+\frac{1}{2}(\nabla\Phi_2)^2+f_2(t)\right\}. \quad (1)$$

The continuous condition of normal velocity can be written as

$$-\frac{\partial F}{\partial t}=\nabla\Phi_1\cdot\nabla F=\nabla\Phi_2\cdot\nabla F. \quad (2)$$

Where ρ_i is density, Φ_i is velocity potential, $f_i(t)$ is an arbitrary function only relying on time. Physical quantity of one side of the interface is denoted by the subscript '1' and the other is '2'.

Let $y=0$ be the unperturbed surface. Considering two layer fluid ($y>0$ and $y<0$) each with a finite velocity along x direction respectively and ignoring a potential field, we can write such velocity potential as

$$\Phi_i=u_i^{(0)}x+\varphi_i(x,t). \quad (3)$$

Where $\varphi_i(x,t)$ is the perturbation of velocity potential.

Expanding φ_i at the unperturbed interface ($y=0$) and substituting it into the boundary conditions (1) and (2), we obtain

$$\begin{aligned}\eta_t &= -\eta_x u_1^{(0)}-\varphi_{1x}\eta_x+\varphi_{1y}+\varphi_{1yy}\eta\\ &= -\eta_x u_2^{(0)}-\varphi_{2x}\eta_x+\varphi_{2y}\\ &\quad+\varphi_{2yy}\eta\rho_1\Big\{\varphi_{1t}+\varphi_{1ty}\eta+u_1^{(0)}\varphi_{1x}\\ &\quad+u_1^{(0)}\varphi_{1xy}\eta+\frac{1}{2}(u_1^{(0)2}+\varphi_{1x}^2+\varphi_{1y}^2)\Big\}\\ &= \rho_2\Big\{\varphi_{2t}+\varphi_{2ty}\eta+u_2^{(0)}\varphi_{2x}\\ &\quad+u_2^{(0)}\varphi_{2xy}\eta+\frac{1}{2}(u_2^{(0)2}+\varphi_{2x}^2+\varphi_{2y}^2)\Big\}. \quad (4)\end{aligned}$$

Velocity φ_i and position of interface $\eta(x,t)$ are expanded by a small number ε, i.e.

$$\begin{aligned}\varphi_i&=\varepsilon\varphi_i^{(1)}+\varepsilon^2\varphi_i^{(2)}+O(\varepsilon^3),\\ \eta&=\varepsilon\eta^{(1)}+\varepsilon^2\eta^{(2)}+O(\varepsilon^3). \quad (5)\end{aligned}$$

Substituting Eq.(5) into Eq.(4), comparing the same rank, we obtain the following equation:

First-order equations, at $y=0$ are

$$\begin{aligned}&\eta_t^{(1)}=-u_1^{(0)}\eta_x^{(1)}+\varphi_{1y}^{(1)}=-u_2^{(0)}\eta_x^{(1)}+\varphi_{2y}^{(1)},\\ &\rho_1\left\{\varphi_{1t}^{(1)}+u_1^{(0)}\varphi_{1x}^{(1)}\right\}=\rho_2\left\{\varphi_{2t}^{(1)}+u_2^{(0)}\varphi_{2x}^{(1)}\right\}, \quad (6)\end{aligned}$$

Second-order equations, at $y=0$ are

$$\begin{aligned}\eta_t^{(2)} &= -u_1^{(0)}\eta_x^{(2)}-\varphi_{1x}^{(1)}\eta_x^{(1)}+\varphi_{1y}^{(2)}+\varphi_{1yy}^{(1)}\eta^{(1)}\\ &= -u_2^{(0)}\eta_x^{(2)}-\varphi_{2x}^{(1)}\eta_x^{(1)}+\varphi_{2y}^{(2)}+\varphi_{2yy}^{(1)}\eta^{(1)},\\ &\rho_1\Big\{\varphi_{1t}^{(2)}+\varphi_{1ty}^{(1)}\eta^{(1)}+u_1^{(0)}\varphi_{1x}^{(2)}\\ &\quad+u_1^{(0)}\varphi_{1xy}^{(1)}\eta^{(1)}+\frac{1}{2}(\varphi_{1x}^{(1)2}+\varphi_{1y}^{(1)2})\Big\}\\ &= \rho_2\Big\{\varphi_{2t}^{(2)}+\varphi_{2ty}^{(1)}\eta^{(1)}+u_2^{(0)}\varphi_{2x}^{(2)}\\ &\quad+u_2^{(0)}\varphi_{2xy}^{(1)}\eta^{(1)}+\frac{1}{2}(\varphi_{2x}^{(1)2}+\varphi_{2y}^{(1)2})\Big\}. \quad (7)\end{aligned}$$

All the orders of φ_i satisfy the Laplace equation.

Typical initial perturbations are a superposition of modes. Given the initial perturbation conditions, we can solve these equations. In linear phase, first-order equation (6) can describe the development of mode coupling accurately. In weakly phase, the second-order equation (7) can describe the development of mode coupling approximately. In nonlinear phase, analytic theory is difficult to describe the development of mode coupling. Numerical simulation is one of the main methods for researching into nonlinear mode coupling KH instability.

3. Numerical methods

The finite difference hydrodynamic code LARED-S[22−24] is used in numerical simulation. The hydrodynamic equations in LARED-S are integrated with the flux-corrected transport (FCT) algorithm in space and the second-order Runge-Kutta method in time. The FCT with sixth-order accurate phase error is used and has second-order accuracy on the uniform part of the grid.

We initial each mode at time $t=0$ by taking an interface perturbation of the form

$$\eta(x,y,0)=\eta_0\cos(kx) \quad (8)$$

and apply periodic boundary conditions at x direction. Where k is the wave number ($k=2\pi/\lambda=2\pi\cdot l$) and η_0 is the initial perturbation amplitude. The initial interface is at $y=0$. We always use a mesh in which the smallest initial perturbation wavelength includes at least 40 mesh points.

We analyse the spectrum by first calculating the vertical density Integral $\int\rho(x,y)\mathrm{d}y$, and then we take the discrete Fourier transform. This procedure gives an accurate representation of the interface at initial times. We believe that it is also valid at relatively late times, so long as the flow has not developed into a turbulent regime (as will be demonstrated in the results presented below).

4. Mode–mode interactions

Here we investigate cases with two initial perturbation modes. We give two examples: one with similar wavelengths (short-range interactions in k space) and one with dissimilar wavelengths (long-range interactions).

The growth of instability mode comes from two aspects. One is the growth of its own and the other is the growth of mode coupling. We assume that there are two linear growing waves with wave numbers k_A and k_B at the initial time. Mode coupling between the two waves excites many waves with wave numbers $k = k_A \pm k_B$, $2k_A$ and $2k_B$.

4.1. Interaction of nearby modes

First we examine the case where the initial perturbation consists of the two nearby modes: $l = 4$ and $l = 5$, representing the interaction of similar wavelengths. Mode coupling between the $l = 4$ and $l = 5$ modes will couple $l = 8$, $l = 10$, $l = 1$ and $l = 9$ modes. The initial perturbation amplitudes are $0.32\,\mu m$ for $l = 4$ and $0.21\,\mu$m for $l = 5$. In Figs.1(a)–1(f) we plot the Fourier spectrum of the interface, superposed with the spectra of single-mode calculations for $l = 4$ and $l = 5$, at six increasing times and in Figs.1(g)–1(l) we plot the outline of the corresponding physical space at the same times. Notice that at early times the growth is nearly without interaction: each mode grows at the same rate as that when it is alone. At later times, the flow enters the nonlinear regime. It is clear that the $l = 4$ mode (which initially had the higher amplitude) is significantly reduced in amplitude (in comparison with its growth as a single mode) although the flow still seems ordered, while $l = 5$ is affected to a much lesser extent. This is seen in the spectrum (Fig.1(e)), showing that indeed the $l = 5$ periodicity is dominant. At still later times we see that the interface lacks of accurate local periodicity (which characterizes a single-mode flow), and the flow takes on a more turbulent nature.

We find it instructive to emphasize the following points regarding the interaction of similar modes. (1) The $l = 8$ mode and $l = 10$ mode grow rapidly in single-mode calculations. But in two modes ($l = 4$ and $l = 5$) coupling calculations, these two modes ($l = 8$ and $l = 10$) manifest contrarily. The growth rate of $l = 9$ mode is larger than those of the $l = 8$ and $l = 10$ modes. (2) At last stage, the amplitude of difference frequency ($l = 1$ mode) mode and sum frequency mode ($l = 9$ mode) is dominant.

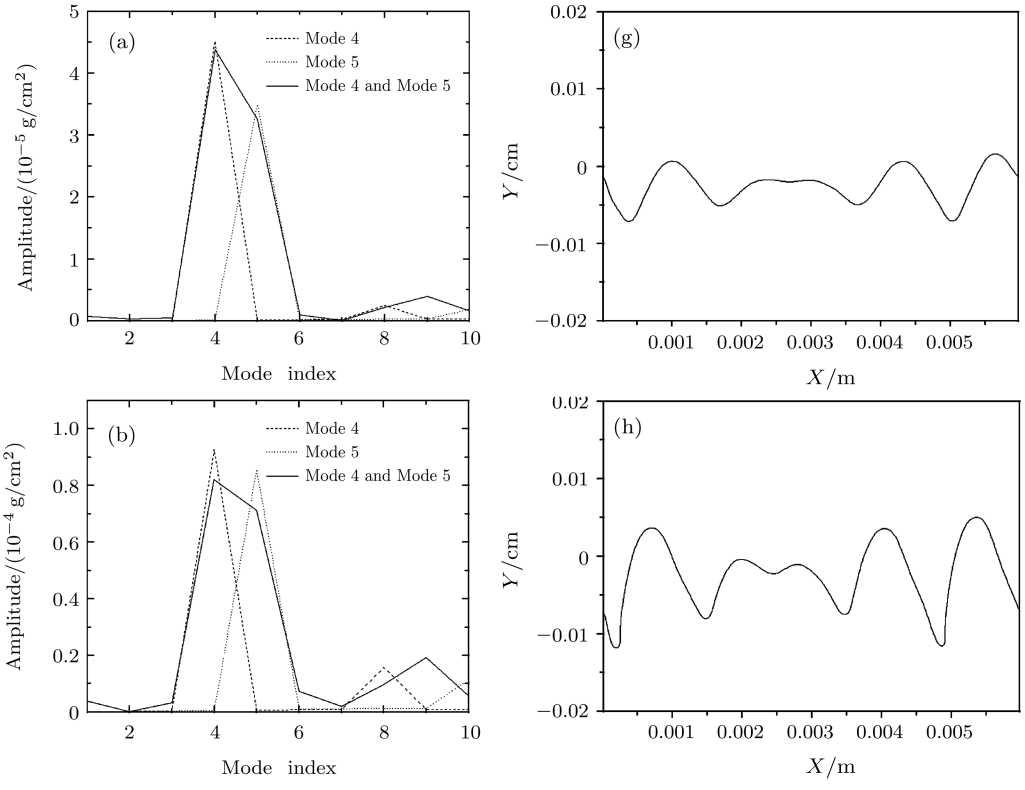

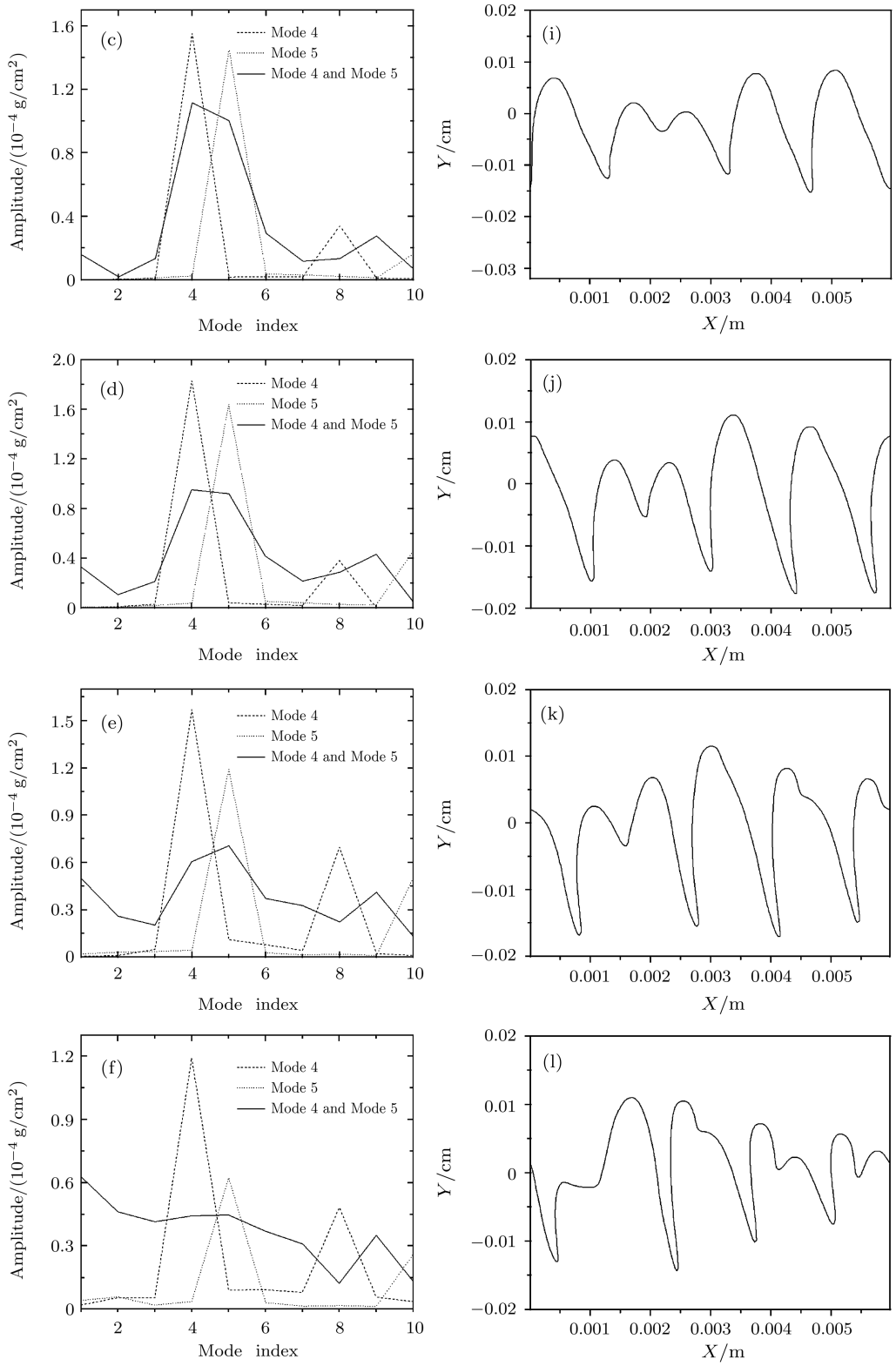

Fig.1. Evolution of a two-mode case with $l = 4$ and $l = 5$ (I indicates the number of wavelengths). Initial perturbation amplitudes are 0.32 μm for $l = 4$ and 0.21 μm for $l = 5$. Parts (a)–(f) depict the interface spectrum at $T = 0.2$ ns, 0.4 ns, 0.6 ns, 0.8 ns, 1.0 ns, 1.2 ns, respectively, and parts (g)–(l) show the physical interface at the same times.

4.2. Interaction of dissimilar modes

To further illustrate the above points, we conducted a second set of calculations for the modes $l = 2$ and $l = 6$, attempting to study the interaction of modes with different wavelength scales. In Fig.2 we plot the results of these calculations for both physical interfaces and spectra. Initial perturbation amplitudes are $0.32\,\mu$m for $l = 2$ and $0.16\,\mu$m for $l = 6$. Again there are three distinct stages: early times where growth is linear; intermediate times where the flow is still rather ordered but strong interaction between modes exists; finally, the flow becomes turbulent with a large number of modes that were not present in the initial conditions.

Notice that at early times the growth is nearly without interaction: each mode grows at the same rate as that when it is alone. At later times, the flow enters the nonlinear regime. It is clear that the $l = 2$ mode (which initially had the higher amplitude) is significantly reduced in amplitude (in comparison with its growth as a single mode) although the flow still seems ordered, while $l = 6$ is affected to a much lesser extent. This is seen in the spectra (Figs.1(a)–1(e)), showing that indeed the $l = 6$ periodicity is dominant. At still later times, it is clear that the $l = 6$ mode is significantly reduced in amplitude (in comparison with its growth as a single mode), while $l = 2$ is affected to a lesser extent. This is seen in the spectrum (Figs.1(f)), showing that indeed the $l = 2$ periodicity is dominant. At still later times we see that the interface also has accurate local periodicity, and the flow takes on a more turbulent nature.

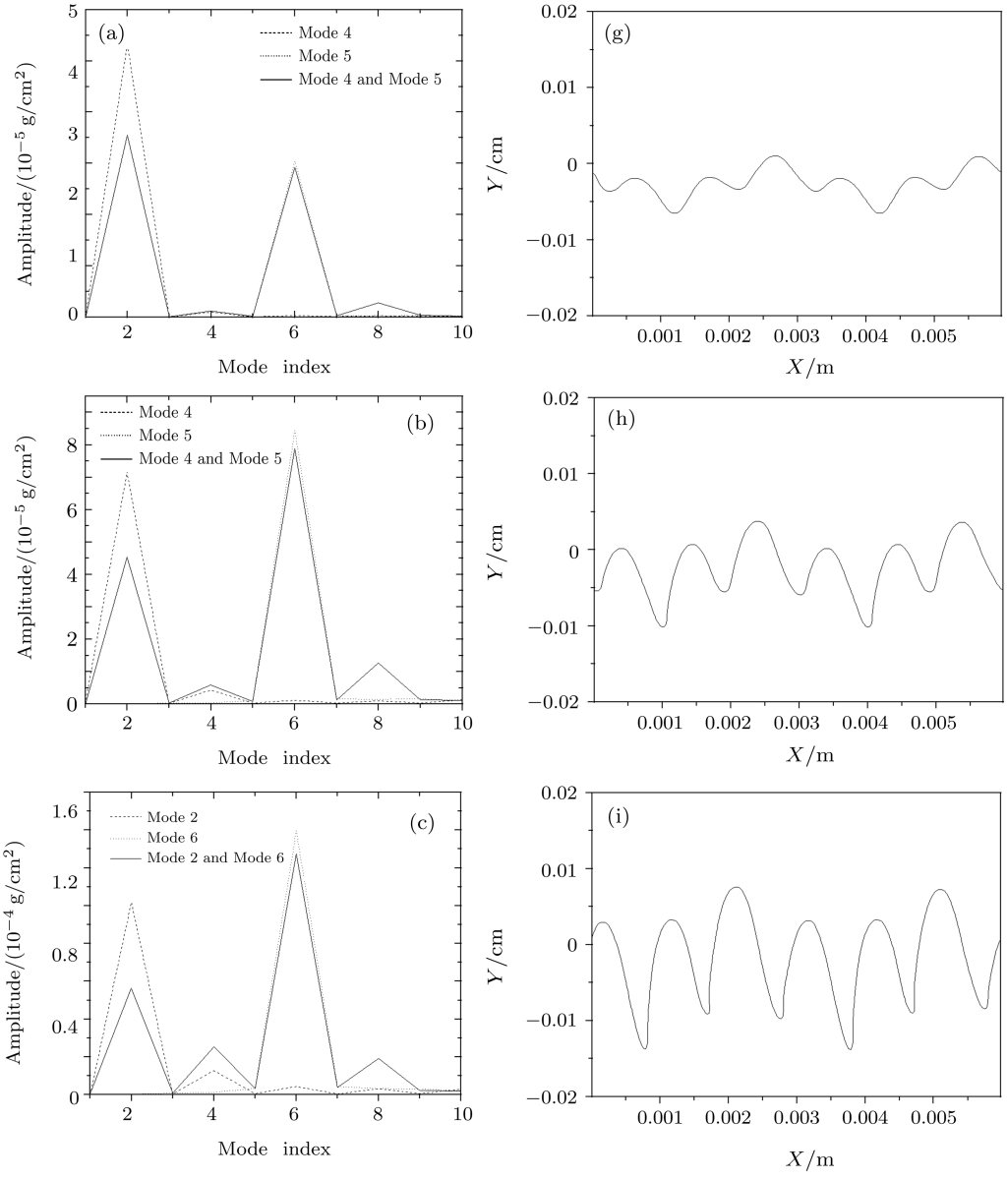

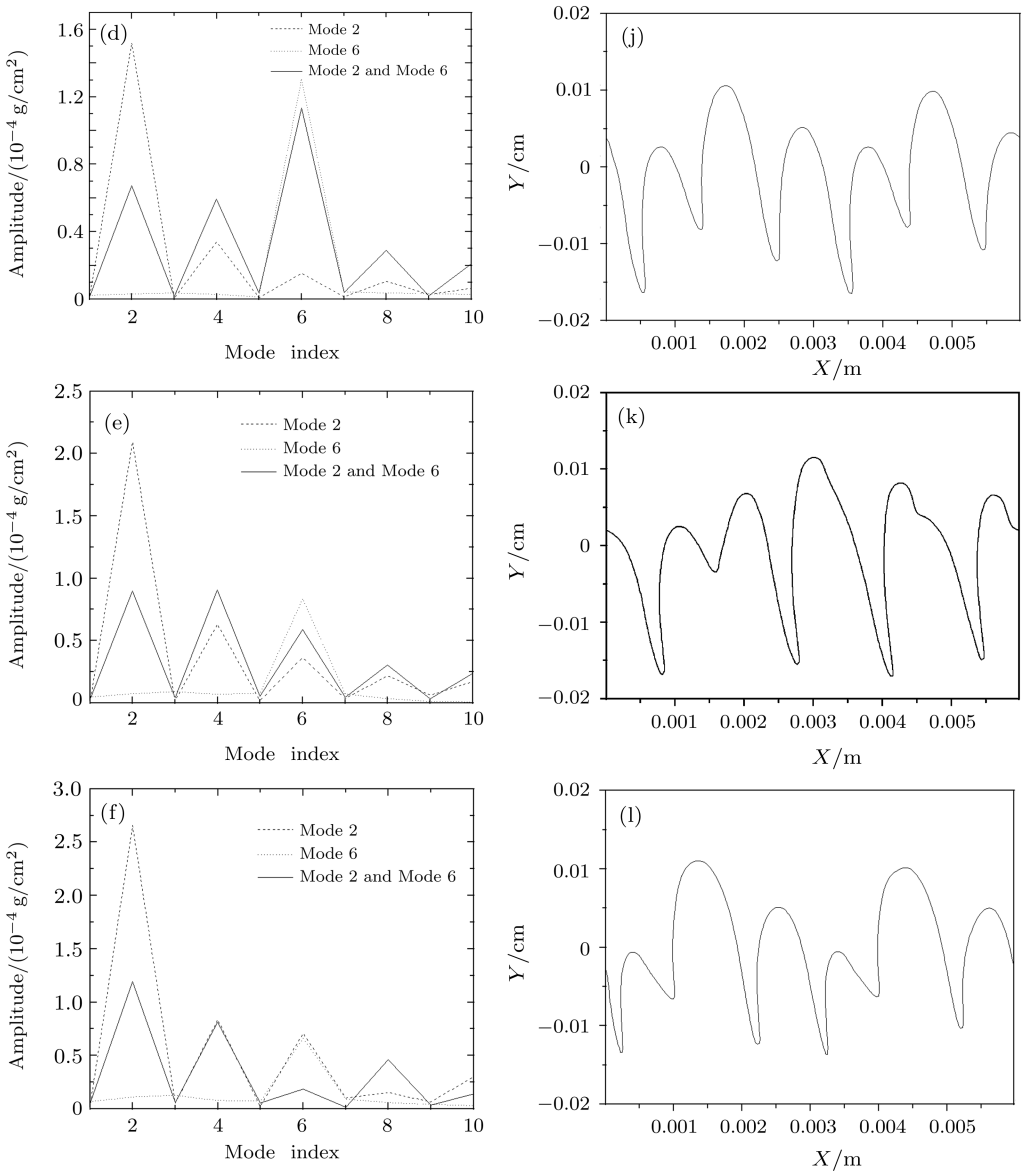

Fig.2. Evolution of a two-mode case with $l = 2$ and $l = 6$ (I indicates the number of wavelengths). Initial perturbation amplitudes are $0.32\,\mu$m for $l = 2$ and $0.16\,\mu$m for $l = 6$. Parts (a)–(f) depict the interface spectrum at $T = 0.2$ ns, 0.4 ns, 0.6 ns, 0.8 ns, 1.0 ns,1.2 ns, respectively, and parts (g)–(l) show the physical interface at the same times.

We find it instructive to emphasize the following points regarding the interaction of dissimilar modes. (1) At the onset of interaction, one mode is suppressed whereas the other continues growth according to its single-mode dynamics. This suggests a nonsymmetric transition to "nonlinearity," i.e., the relative effect of the interaction on the various modes is unequal. This seems to indicate that there is no simple equivalent transformation from a band of similar modes to one mode representing their effective amplitude. (2) At early time the $l = 2$ periodicity is dominant; at later time the $l = 6$ periodicity is dominant. This phenomenon is novel.

5. Summery

In phase II, mode–mode interaction is still ordered and the presence of one mode can suppress the amplitude of another mode. We emphasize that although this stage clearly includes mode–mode interaction, it can occur when one or both modes have an amplitude that is clearly still in the classical single-mode 'linear' regime. There is no simple equivalent transformation from a band of similar modes to one mode representing their effective amplitude. In phase III, the random or 'turbulent' stage, mode coupling develops towards low-l modes.

The results we bring here should be significant in understanding the stages of the development of multi-mode KH instability, since in most physical cases the flow cannot be described by a single mode.

References

[1] Chandrasekhar S 1961 *Hydrodynamic and Hydromagnetic Stability* (London: Oxford University Press) Chap. **10**

[2] Hasegawa1 H, Fujimoto M, Phan T D, Reme H, Balogh A, Dunlop M W, Hashimoto C and TanDokoro R 2004 *Nature* **430** 755

[3] Lobanov A P and Zensus J A 2001 *Science* **294** 128

[4] Zinnecker H, McCaughrean M J and Rayner J T 1998 *Nature* **394** 862

[5] Gamexo V N, Khokhlo A M, Oran E S, Almadena Y C and Robert O R 2003 *Science* **299** 77

[6] Burrows A 2000 *Nature* **430** 727

[7] Nomoto K, Iwamoto K and Kishimoto N 1997 *Science* **276** 1378

[8] Price D J and Rosswog S 2006 *Science* **312** 719

[9] Nayffh A H and Saric W S 1970 *J. Fluid Mech.* **46** 209

[10] Walker J S 1993 *Phys. Fluids* A **5** 1466

[11] Bau H H 1982 *Phys. Fluids* **25** 1719

[12] Tauber W, Unverdi S O and Tryggvason G 2002 *Phys. Fluids* **14** 2871

[13] Keskinen M J 1995 *Phys. Plasmas* **3** 1259

[14] Drazin P G 1969 *J. Fluid Mech.* **42** 321

[15] Bodo G 2004 *Phys. Rev.* E **70** 36304

[16] Miura A 1999 *Phys. Rev. Lett.* **83** 1586

[17] Horton W, Perez J C, Carter T and Bengtson R 2005 *Phys. Plasmas* **12** 22303

[18] Lawrence G A, Browand F K and Redekopp L G 1991 *Phys. Fluids* A **3** 2360

[19] Baty H, Keppens R and Comte P 2003 *Phys. Plasmas* **10** 4661

[20] Rangel R H and Sirignano W A 1988 *Phys. Fluids* **31** 1845

[21] Ye W H, Zhang W Y and He X T 2002 *Phys. Rev.* E **65** 57401

[22] Ye W H, Zhang W Y and He X T 2000 *Acta Phys. Sin.* **49** 762 (in Chinese)

[23] Wu J F, Ye W H, Zhang W Y and He X T 2003 *Acta Phys. Sin.* **52** 1688 (in Chinese)

[24] Knauer J P 2000 *Phys. Plasmas* **7** 338